Journal of Theoretical and Applied Information Technology
31st May 2023. Vol.101. No 10

ISSN: 1992-8645 www.jatit.org E-ISSN: 1817-3195

# PATHOLOGY CARDIAC MONITORING STUDY OF THE PHONOCARDIOGRAM SIGNAL

**DEBBAL IMANE[1], HAMZA CHERIF LOTFI[2], BAAKEK YETTOU NOUR EL HOUDA[3]**

[1,2,3] *Genie* Biomedical Laboratory (GBM), Faculty of Technology, University Abou Bakr Belkaid Tlemcen,

Genie Biomedical department, Algeria

E-mail: [1]Imane.debbal@univ-tlemcen.dz, [2]Lotfi.hamzacherif@univ-tlemcen.dz, [3]nourelhouda.baakekyettou@univ-tlemcen.dz

**ABSTRACT**

In this paper, we will discuss the efficiency of the Fast Fourier transform (FFT) and the Short-Time Fourier Transform (STFT) to distinguish cardiac pathological signals, along with following the severity evolution of diverse diseases through three selected features. The cardiac signals analysed and previously classified via some clinical data will be arranged into three main classes or groups: a group of signals containing neither clicks nor murmurs and having a similar morphology, a second group of signals containing only clicks (reduced murmurs), and a third group of signals with a significant murmur. The features that we are going to define from each technic will help us in this sense to classify the different signals analysed in one of the mentioned groups. We will then extract the same features from a fourth group of phonocardiogram (PCG) signals suffering from murmur with different severity levels. In the end, we will discuss the accuracy of these features with the Energetic Ratio (ER) parameter and a K-Nearest Neighbor classifier in terms of classifying phonocardiogram (PCG) signals according to their pathological origin and cardiac severity level. An accuracy of 99.2% is achieved when using a combination of time and spectral features (frequency band (FB), frequency extent (ΔF), time extent (ΔT)) to classify the PCG signals in the three main groups and a 98.9% accuracy when ranking signals according to their severity level (Light, Moderate, Severe).

The main aim of this paper is to proceed with the use of the FFT and the STFT technics to obtain information likely not only to discriminate the three groups' cases but also to detect the level (or degree) of severity in the same studied pathology as well. Thus, the intent of this study on phonocardiogram (PCG) signals is to follow the evolution of the pathology at different levels and identify each severity degree via the extracted features, which makes the originality of this paper. These results can only help the clinician to make his decision with serenity.

**Keywords:** *Phonocardiogram, Normal, Pathological, Classification, Discrimination, Severity, FFT, STFT, Spectral, Time Extency, Frequency Extency.*

## 1. INTRODUCTION

A phonocardiogram (PCG) is a scheme for emulating high precision copy of the sounds made by the heart along with the murmurs made during the procedure of pumping blood [1]. The cardiac signals recorded via a phonocardiograph may reflect divers' pathological conditions of cardiovascular system that being the case for why several researchers focus on heart sounds analysis (acquisition, signal processing, segmentation and feature extraction from different PCG cycles).

Under normal conditions, two heart sounds can be distinguish on the graphic representation of the recorded phonocardiogram (PCG). The first heart sound known also as heartbeat S1, corresponding to the beginning of ventricular systole, is the result of the closure of the mitral and tricuspid valves [2]. While the second heartbeat S2, referring to the end of the ventricular systole and marking the beginning of the diastole, is associated with the closure of the aortic and pulmonic valves [2]. Other than S1 and S2, murmurs and short murmurs (clicks) appears indicating abnormal heart condition. Murmurs are sounds resulting from certain cardiovascular diseases that are audible during the systole, the diastole, or both [3][4].

Stenosis and regurgitation are the two ailments who relate to the opening and the closing of the valves detected by analysing the PCG signal [1]. Therefore the algorithms used for cardiac signals processing is more on a quantitative, precise and objective

Journal of Theoretical and Applied Information Technology
31st May 2023. Vol.101. No 10

ISSN: 1992-8645 www.jatit.org E-ISSN: 1817-3195

interpretation of heart sounds [5], improving the process of cardiovascular diagnosis. Beyond this, computer-assisted auscultation allows the detection of pathologies who are unrecognized through a conventional auscultation [6].

Hence, researchers used numerous signal-processing tools on PCG recordings for various purposes. Many denoising algorithms have been proposed such as parameter extraction using Discrete Wavelet Transform (DWT) [7], DWT decomposition level exploitation [8-10], Empirical Mode Decomposition [11].

In another study, Baakek et al. conducted a comparative study to highlight the impact of clicks and murmurs on heart sound using an STFT spectrogram [12]. The power spectrum was obtained using FFT analysis, later employed as a feature to classify and discriminate the PCG signals database [13]. In [14], the authors applied an FFT and STFT algorithm on divers PCG signals and used the FFT spectrum to identify the heart sound component as a first step, then extracted the frequency extent of both heart sound 1 (S1) and heart sound 2 (S2). To affirm which of the heart sounds is concerned by the pathology and which of their component is directly affected. The frequency extend values extracted from the STFT spectrogram, discriminated between diastolic and systolic murmur of the studied cardiac pathologies. Hence, these murmurs did not considerably affect the time-frequency content of the sounds S1 and S2.

In this paper, we are focusing on the efficiency of the frequency feature of the Fast Fourier Transform (FFT) and the time-frequency characteristics of the Short-Time Fourier Transform (STFT) to classify different cardiac signals, in one of three pre-established phonocardiogram groups and then study the ability of these characteristics to follow the evolution of the pathology. Therefore, our database classified via some clinical data will be arranged into three main classes or groups: a group of signals containing neither clicks nor murmurs and having a similar morphology, a second group of signals containing only clicks (reduced murmurs), and a third group containing signals with large murmurs. The first step of this work will be to analyse the PCG signals with the FFT and STFT technics. Then, follow with feature extraction (frequency band, time extent, frequency extent) and an Energetic Ratio (ER) parameter comparison / K-Nearest Neighbor (KNN) classification process.

We will proceed with the same analysis on a fourth group containing PCG signals with different severity levels of the same pathology. The obtained results will be used in a KNN classifier to classify the fourth group signals into three classes according to their severity level. Plus, an ER parameter comparison to appreciate the features' variation and evolution.

One of the limitations of this analysis is the possibility of the extracted features to classify the pathological signals of the first group in the second group. Since some of the first group signals are morphology similar to a healthy PCG signal. Yet, their frequency information may be affected by the pathology. The second limitation is the inability of these features to separate close severity levels, which may lead to an incorrect classification and a rather affected accuracy value.

In the end, the correlation of these features with the ER parameter helps us find a plausible medical explanation for the features' variation and evolution.

## 2. MATERIALS AND METHODS

### 2. 1 PCG signals database

Based on clinical data, we can classify the PCG signals into four distinct groups (Table1):

- Group 1 (G1): PCG signals having neither click (reduced murmur) nor significant murmur.
- Group 2 (G2): PCG signals with clicks.
- Group 3 (G3): PCG signals with clicks or murmurs.
- Group 4 (G4): PCG signals with murmurs including different severity levels.

We aim through this study to obtain relevant parameters able to classify our signals into the three main groups and follow the evolution of the cardiac pathology concerned.

The diagram below (Figure 1) illustrates how we proceeded with this study. The relevant parameters calculated during the features extraction step will be introduced into a KNN classifier for a multi-class classification. In addition to that, we used the energy rate parameter (or energetic ratio) ER, since recognised by researchers as a predominant element for pathology monitoring, to compare our results with. We implemented the same program mentioned by previous papers using this parameter for similar research purposes.

We also checked the accuracy of the ER parameter with a KNN classifier to see if it is efficient for this paper' purposes. The classification process consists of classifying the PCG signals into the three main groups as a first step and then classifying the fourth

Journal of Theoretical and Applied Information Technology
31st May 2023. Vol.101. No 10

ISSN: 1992-8645 www.jatit.org E-ISSN: 1817-3195

group of PCG signals into three classes according to their severity level (light, moderate, severe).

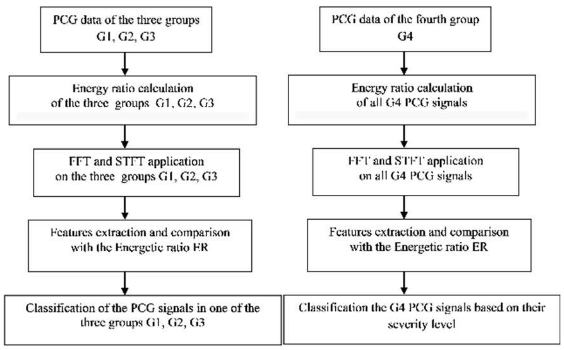


*Figure1. Flow Diagram of features extraction on PCG signals and comparison of pathological severity using the FFT and STFT technic*

The table 1 below defines the PCG signals of the four groups (G1, G2, G3 and G4) used for detecting cardiac pathological differences.

*Table1 PCG signals used for the four groups*

| **PCG signals Group1 (G1)** | Abbreviation | **PCG signals Group2 (G2)** | Abbreviation |
|---|---|---|---|
| Normal heartbeat cardiac sound | N | Ejection click | EC |
| Innocent murmur | IM | Early aortic stenosis | Eas |
| Coarctation of the aorta | Coa | Late systolic | LS |
| | | Aortic gallop | AG |
| **PCG signals Group3 (G3)** | Abbreviation | **PCG signals Group4 (G4)** | Abbreviation |
| Systolic pulmonary Stenosis | PS | Aortic stenosis | As1,As2, As3,As4 |
| Aortic regurgitation | Ar | Mitral stenosis | Ms1,Ms2 ,Ms3,Ms4 |
| Tricuspid regurgitation | Tr | Mitral regurgitation | Mr1,Mr2, Mr3,Mr4 |

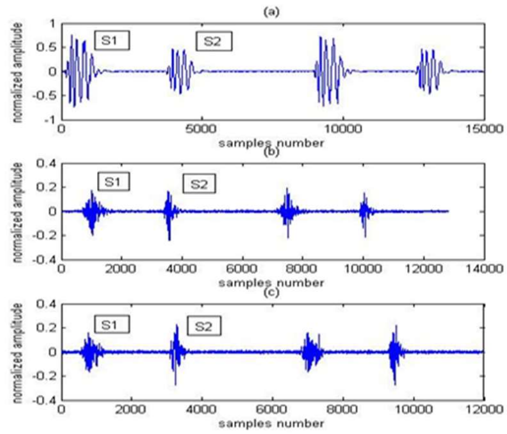


*Figure2. Time representation of a two cycles PCG signals of the group1 (a) the normal signal (N), (b) the innocents murmur signal (IM),(c) the coarctation of the aorta signal (coa).*

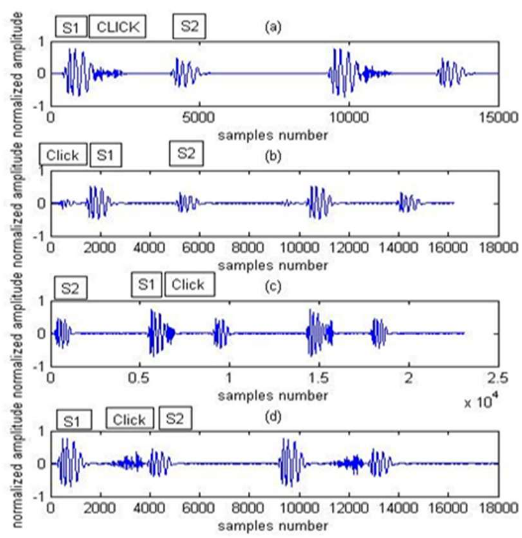


*Figure3. Time representation of a two cycles PCG signals of the group2 (a) the early aortic stenosis signal (Eas),*
*(b) the aortic gallop signal (AG),*
*(c) the ejection click signal (EC),*
*(d) the late systole signal(LS).*

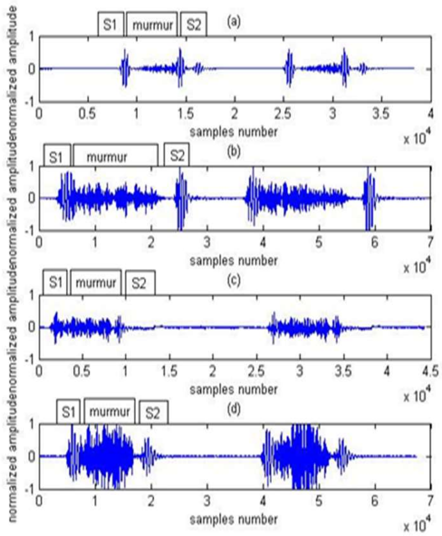


*Figure4. Time representation of a two cycles PCG signals of the group3. (a) the systolic pulmonary stenosis signal (PS), b) the aortic regurgitation signal (Ar), (c) the tricuspid regurgitation signal (Tr), (d) the aortic stenosis signal(As).*

## 2.2 Theoretical background

### 2.2.1 Fast Fourier Transform (FFT)

In 1882, Joseph Fourier discovered that we could represent any periodic function as an infinite sum of periodic complex exponential functions [15]. Later then extended it to any discrete time function. The FT is widely used and usually implemented in the form of FFT algorithm (fast Fourier transform)[16]. The mathematical definition of the FT is given below.

$$X(f) = \int x(t)\, e^{-j2\Pi ft}\, dt \qquad (1)$$

Where t and $f$ are respectively the time and frequency parameters. It defines the spectrum of s(t) which consists of components at all frequencies over the range for which it is non zero [17].

The Fourier Transform (FT) is the most famous and oldest of the transformations used in signal processing fields. During this transformation, the signal is decomposed into a set of basic functions, which are the cosine, the sine, or the imaginary exponential.

The so-called Fourier series decomposition method, consist in decomposing the signal into a sum of sinusoidal function of different frequencies.

The Fourier series is the most used tool to transit from the time domain to the frequency domain. Moreover, a temporal analysis of a signal is often followed by frequency analysis. Since the first representation informs us about the signal's duration and its discontinuities, the second presents the periodicity of the signal.

For the Fourier Transform to exist, the signal must be square summable, i.e of finite energy. For real signals, this condition is always satisfied since the measurement is made over a finite time.

Fourier analysis implicitly assumes that the signal is identical to itself outside the measurement interval. The function (w) being periodic of period T, it is usual to limits its definition to [-T/2, T/2].

Here is one of the properties of the Fourier transform [18], called Parseval identity (conservation of energy independent of any time or frequency variation).

$$\int_{-\infty}^{+\infty} |s(t)|^2 dt = \frac{1}{2\Pi} \int_{-\infty}^{+\infty} |\hat{s}(w)|^2 dw \qquad (1)$$

In general, we can define the Fourier Transform as a linear application which associates N values s(0),…,s(k),…,s(N-1), N other values

$$\hat{s}_0, \ldots\ldots, \hat{s}_n, \ldots\ldots, \hat{s}_{N-1}$$

Defined by:

$$\hat{s}_n = \sum_{k=0}^{N-1} s(k) e^{-j2\Pi kn/N} \qquad (2)$$

$$n \in \{0, \ldots., N-1\}$$

Where N represents the minimum number of samples to be taken to reconstruct the signal s(t). In this case, we will name this transform, discrete Fourier transform. The inverse discrete Fourier transform is written:

$$s(k) = \frac{1}{N} \sum_{n=0}^{N-1} s_n e^{j2\Pi kn/N}, k \in \{0, \ldots., N-1\} \qquad (3)$$

***Sampling***

By definition, a signal s(t) of finite energy whose Fourier transform has bounded support [-B, B], is entirely defined by its samples s(kTe) taken at the sampling frequency fe $\geq 2B$ . The sampling process consists in multiplying the signal s(t) by the sampling function e(t).

$$\tilde{s}(t) = s(t)e(t) = \sum_{k=-\infty}^{+\infty} s(kTe)\delta(t - kTe) \qquad (4)$$

With $\widetilde{s}(t)$ is the sampled signal.

The Fourier Transform is then written as the following

$$\widetilde{\widetilde{s}}(f) = \frac{1}{Te}\sum_{n=-\infty}^{+\infty} s\left[f - \frac{n}{Te}\right] \qquad (5)$$

To prevent the spectrum from folding up to the axes of symmetry, the signal must not contain any frequency higher than fe/2.

**N.B;**

The Fast Fourier Transform (FFT) is an algorithm, which makes it possible to calculate Discrete Fourier Transforms DFT. The DFT appears in many applications in signal processing because of its aptitude to determine the weighting between different discrete frequencies. Therefore, the discrete data taken as input is often called a ***signal,*** and in this case, it is defined in the time domain. The output values are then called the ***spectrum*** and are defined in the frequency domain.

### 2.2.2 Short-time Fourier transforms (STFT)

The STFT consist on calculating the Fourier transform of a sliding windowed version of the time signal s(t). The location of the sliding window adds a time dimension and one gets a time-varying frequency analysis.

The mathematical representation of STFT is:

$$S(t,f) = \int_{-\infty}^{+\infty} s(\tau)w(\tau - t)e^{-j2\pi \ ft}d\tau \qquad (6)$$

Where $w(\tau - t)$ it is the sliding window applied to the signal $s(t)$, $f$ is the frequency and t is the time.

The length of the window is chosen so that to maintain signal stationary in order to calculate the Fourier transform. To reduce the effect of leakage (the effect of having finite duration), each sub-record is then multiplied by an appropriate window and then the Fourier transform is applied to each sub-record. As long as each sub-record does not contain rapid changes the spectrogram will give an excellent idea of how the spectral composition of the signal has changed during the whole time record.[16]

### 2.3 Parameters study and analysing

### 2.3.1Frequency Band

It is the frequency range occupied by one cycle of a PCG signal (Figure 5)

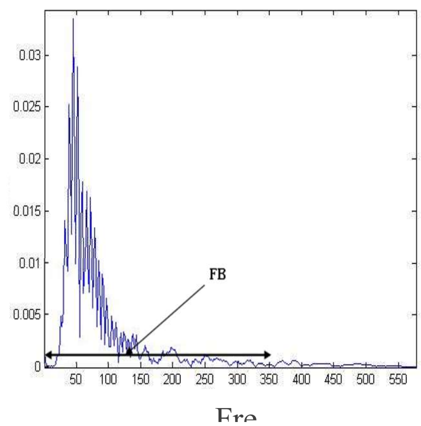


*Figure 5: Illustrate the FB feature of a normal PCG case on an FFT spectral representation.*

### 2.3.2 Temporal extent (Δ*T*) and frequency extent (Δ*F*)

The Figure 6 down below illustrate de definition of these two features.

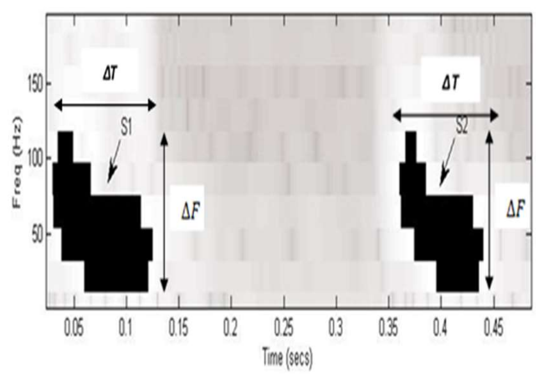


*Figure 6: Illustrate the ΔT and ΔF features on an STFT representation for a normal PCG case*

### 2.3.3 Energetic Ratio (ER)

Used in this study, as a reference feature to compare the results obtained by using FFT and STFT technic with. Previous research mentioned that the ER is very efficient for tracking cardiac disease severity [12, 19][20-27].

The ER provides an idea of the relative energy of cardiac murmurs relative to other heart sounds S1 and S2 [24], which make him important indicators on estimating the degree of heart severity. It is defined as in the equation below [19]

$$ER = \frac{E_2}{E_1 + E_2} \times 100 \qquad (7)$$

**Journal of Theoretical and Applied Information Technology**
31st May 2023. Vol.101. No 10

ISSN: 1992-8645 www.jatit.org E-ISSN: 1817-3195

Where E2 is the heart murmur energy, E1 is the energy of S1 + S2 and (E1 + E2) is the total energy. In case ER equals to 100%, we have a complete dominance of the clicks or murmur over the two heart sounds (S1 and S2).

**2.4 Machine learning method**

**2.4.1 K-nearest neighbor**

The main principle of nearest neighbor methods is to find the nearest predetermined number of training samples to the new point and estimate the class. The number of samples -K- is a user-defined constant (k-nearest neighbor learning) or a variable depending on the local density of points [28]. Distance can generally be any metric measure: for example, the standard Euclidean distance is the most common choice. Neighbor-based methods are known as non-generalized machine learning methods and classification is sample-based learning. The classification is calculated by a simple majority vote of each point's nearest neighbors, and a query point is assigned the data class with the most representative among the point's nearest neighbors. [29-31]

The parameter setting of KNN model is shown in Table

Table 2: K-Nearest Neighbor parameter setting

| KNN parameter | Value |
|---|---|
| **Learning rate** | 1e-4 |
| **Number of epoch** | 200 |
| **Neighbours number** | 3 |
| **Distance** | Euclidian |

## 3. RESULTS

Just like illustrated in the diagram (figure1) this work is divided into two parts. The first one is about a classification of pathological severity between the three groups G1, G2, G3, when the seconds aim is to classify the G4 PCG signals based on their severity level.

**3.1 Analysis results of the PCG signals of the four groups (G1, G2, G3 and G4) by using the FFT technique.**

All the tables include the results obtained when implementing the energetic ratio ER program.

Table 3 and table 4 give the results obtained by applying the FFT technique to the four groups (G1, G2, G3 and G4).

The figure 7 represent the FFTs' frequency spectrum of one PCG signal from each group, which we used to extract the frequency band (FB) feature.

Figure 8 holds the obtain results of the frequency band for the three groups of signals.

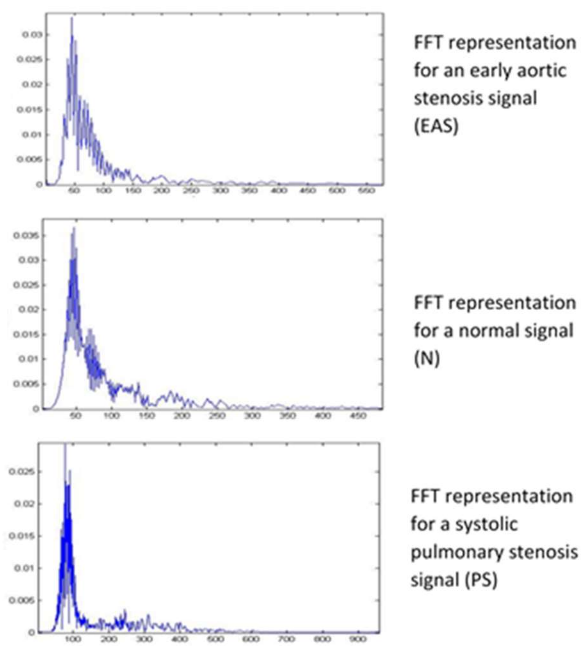


*Figure 7: FFTs' frequency spectrum of one PCG signal from each of the three groups.*

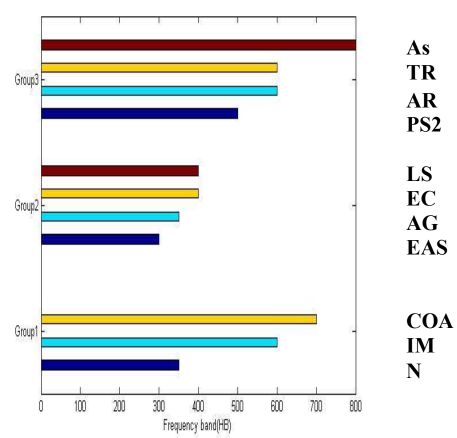


*Figure 8: variation of frequency Band (FB) feature for the three groups (G1, G2 and G3) PCG signals.*

ISSN: 1992-8645 www.jatit.org E-ISSN: 1817-3195

**3.2 Analysis results of the PCG signals of the four groups (G1, G2, G3 and G4) by using the STFT technique.**

Table 6 and table 7 give the results obtained by applying the STFT technic to the four groups (G1, G2, G3 and G4).

Figure 9 and figure 10 give an overview on the application of the STFT technic on the PCG signals (G1 and G4)

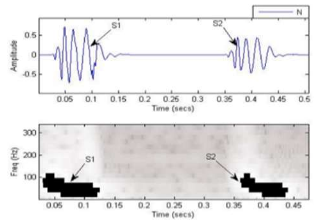

STFTrepresentation for a normal signal (N)

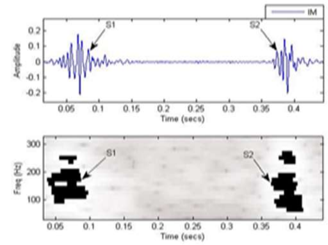

STFT representation for an innocent murmur signal (IM)

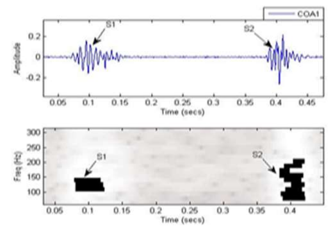

STFT representation for a coarctation of the aorta signal (COA)

*Figure 9: STFT representation for group 1 PCG signals*

*Table 3: variation of frequency band (FB) and energetic ratio (ER) features for the three group PCG signals*

| Features \ signals | One PCG cycle | |
|---|---|---|
| | Energetic Ratio (ER)(%) | Frequency Band (FB) (Hz) |
| PCG signals without clicks nor murmurs | | |
| N | 0 | 0 - 350 |
| IM | 0 | 0 - 600 |
| Coa1 | 0 | 0 - 700 |
| PCG signals with clicks | | |
| EAS | 2.5 | 0 - 300 |
| AG | 2.8 | 0 - 350 |
| EC | 3.9 | 0 - 400 |
| LS | 4.1 | 0 - 400 |
| PCG signals with murmurs | | |
| PS2 | 5.3 | 0 - 500 |
| AR | 38.3 | 0 - 600 |
| TR | 57.8 | 0 - 600 |
| AS | 85.4 | 0 - 800 |

*Table 4: variation of $\Delta T$, $\Delta F$ and the energetic ratio ER features within the three groups*

ISSN: 1992-8645 www.jatit.org E-ISSN: 1817-3195

| Features / signals | Energetic ratio (ER) | S1 | | S2 | | Murmurs | | Click | |
|---|---|---|---|---|---|---|---|---|---|
| | | Temporal Extent $\Delta t$ (sec) | Frequency Extent $\Delta f$ (Hz) | $\Delta t$ (sec) | $\Delta f$ (Hz) | $\Delta t$ (sec) | $\Delta f$ (Hz) | $\Delta t$ (sec) | $\Delta f$ (Hz) |
| PCG signals without clicks nor murmurs | | | | | | | | | |
| N | 0 | 0.11 | 130 | 0.09 | 130 | | | | |
| IM | 0 | 0.08 | 129 | 0.05 | 144 | | | | |
| Coa1 | 0 | 0.04 | 67 | 0.04 | 159 | | | | |
| PCG signals with clicks | | | | | | | | | |
| EAS | 2.5 | 0.15 | 145 | 0.14 | 130 | | | 0.02 | 65 |
| AG | 2.8 | 0.11 | 141 | 0.12 | 128 | | | 0.08 | 85 |
| EC | 3.9 | 0.10 | 135 | 0.12 | 126 | | | 0.08 | 160 |
| LS | 4.1 | 0.10 | 129 | 0.12 | 110 | | | 0.1 | 200 |
| PCG signals with murmurs | | | | | | | | | |
| PS2 | 5.3 | 0.07 | 140 | 0.08 | 136 | 0.22 | 215 | | |
| AR | 38.3 | 0.07 | 235 | 0.06 | 136 | 0.27 | 301 | | |
| TR | 57.8 | 0.06 | 287 | 0.05 | 287 | 0.30 | 345 | | |
| AS | 85.4 | 0.05 | 416 | 0.04 | 374 | 0.35 | 517 | | |

*Table 5: Variation of FB and ER features within the fourth group of signals*

| Features / signals | One PCG Cycle | |
|---|---|---|
| | Energetic Ratio (ER) (%) | Frequency Band FB (Hz) |
| PCG signals with diastolic murmurs | | |
| Mitral Stenosis | | |
| MS1 | 12 | 0 - 600 |
| MS2 | 40 | 0 - 550 |
| MS3 | 76 | 0 - 500 |
| MS4 | 85 | 0 - 450 |
| PCG signals with systolic murmurs | | |
| Aortic Stenosis | | |
| AS1 | 55 | 0 - 550 |
| AS2 | 93 | 0 - 450 |
| AS3 | 94 | 0 - 400 |
| AS4 | 95 | 0 - 300 |
| Mitral Regurgitation | | |
| MR1 | 14 | 0 – 1300 |
| MR2 | 24 | 0 – 1200 |
| MR3 | 56 | 0 – 950 |
| MR4 | 75 | 0 – 950 |

ISSN: 1992-8645 www.jatit.org E-ISSN: 1817-3195

*Table 6: Variation of $\Delta T$, $\Delta F$ and ER features within the fourth group signals (Mitral stenosis (MS) aortic stenosis (AS and mitral regurgitation (MR)).*

| Features / Signals | Energetic ratio (ER) | S1 | | S2 | | murmurs | |
|---|---|---|---|---|---|---|---|
| | | Temporal extent $\Delta t$ (sec) | Frequency extent $\Delta f$ (Hz) | $\Delta t$ (sec) | $\Delta f$ (Hz) | $\Delta t$ (sec) | $\Delta f$ (Hz) |
| PCG signals with diastolic murmurs | | | | | | | |
| Mitral Stenosis | | | | | | | |
| Ms1 | 12 | 0.04 | 131 | 0.15 | 480 | 0.16 | 411 |
| Ms2 | 40 | 0.08 | 285 | 0.13 | 431 | 0.30 | 110 |
| Ms3 | 76 | 0.08 | 285 | 0.08 | 256 | 0.22 | 90 |
| Ms4 | 85 | 0.09 | 215 | 0.08 | 225 | 0.05 | 87 |
| PCG signals with systolic murmurs | | | | | | | |
| Aortic Stenosis | | | | | | | |
| As1 | 55 | 0.01 | 140 | 0.02 | 250 | 0.25 | 600 |
| As2 | 93 | 0.04 | 258 | 0.03 | 275 | 0.26 | 480 |
| As3 | 94 | 0.07 | 330 | 0.03 | 300 | 0.26 | 460 |
| As4 | 95 | 0.07 | 340 | 0.05 | 310 | 0.28 | 300 |
| Mitral regurgitation | | | | | | | |
| Mr1 | 14 | 0.09 | 105 | 0.06 | 128 | 0.28 | 160 |
| Mr2 | 24 | 0.09 | 107 | 0.06 | 111 | 0.28 | 323 |
| Mr3 | 56 | 0.07 | 135 | 0.05 | 110 | 0.17 | 352 |
| Mr4 | 75 | 0.07 | 172 | 0.05 | 86 | 0.17 | 452 |

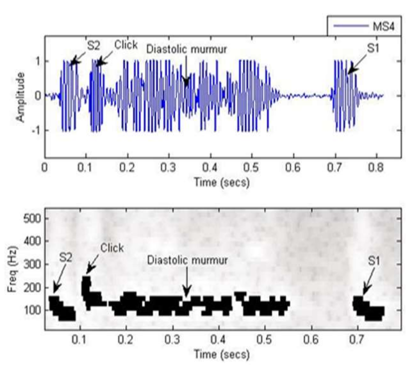


Temporal and STFT representation
for the MS4 signal

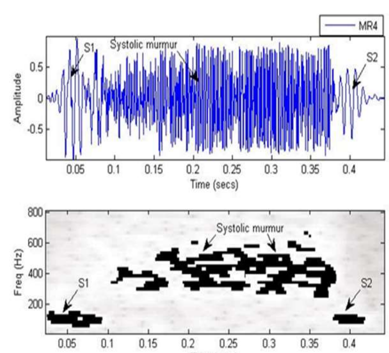


Temporal and STFT representation
for the MR4 signal

*Figure 10: Temporal and STFT representation for one of the MS (Mitral Stenosis) and MR (Mitral Regurgitation) signals.*

Journal of Theoretical and Applied Information Technology
31st May 2023. Vol.101. No 10

ISSN: 1992-8645 www.jatit.org E-ISSN: 1817-3195

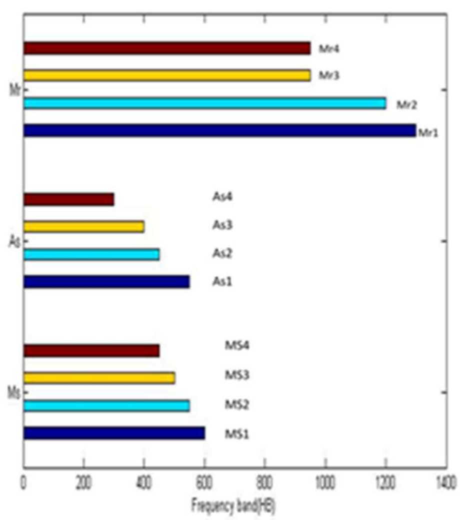


*Figure 11: variation of the frequency band (FB) feature for the fourth group PCG signals: mitral stenosis (MS), aortic stenosis (AS), mitral regurgitation (MR);*

### 3.3 Machine learning results

This classification will help us check the efficiency of the FFT and the STFT features to classify the database into the three main groups previously rearranged according to clinical data:

- Group 1 (G1): PCG signals having neither click (reduced murmur) nor significant murmur.
- Group 2 (G2): PCG signals with clicks.
- Group 3 (G3): PCG signals with clicks or murmurs.

Table 7 summarizes the performances of the KNN classifier to rearrange the database signals into the three groups using frequency and time-frequency features.

*Table 7: performance table of the KNN classifier into the three main group*

| Performance | Accuracy | Sensitivity | specificity |
|---|---|---|---|
| **Values** | 99.2% | 98.2% | 99.4% |

We also proceeded with a new KNN classification for the fourth group PCG signals. This time, the classification consisted on ranking the fourth group signals into three classes according to their severity level (light, moderate, severe).

*Table 8: performance table of the KNN classifier into three severity levels*

| Performance | Accuracy | Sensitivity | specificity |
|---|---|---|---|
| **Values** | 98.9% | 97.9% | 99.1% |

To evaluate the accuracy of the Energetic ratio ER parameter for this paper' purposes, we proceeded with the same classification process than the FFT and STFT, but with the ER values as a classification feature.

*Table 9 : performance table of the KNN classifier in the three main groups using the energetic ratio ER.*

| Performance | Accuracy | Sensitivity | specificity |
|---|---|---|---|
| **Values** | 99.5% | 98.5% | 99.7% |

*Table 10: performance table of the KNN classifier into three severity levels using the energetic ratio ER.*

| Performance | Accuracy | Sensitivity | specificity |
|---|---|---|---|
| **Values** | 98.8% | 97.8% | 99% |

## 4. DISCUSSION

### 4.1 Comparison of pathological severity between the three groups (G1, G2 and G3)

We applied the Fast Fourier Transform (FFT), the Short-Time Fourier Transform (STFT) and the Energetic Ratio (ER) algorithms on the three groups of PCG signals. In this section, we will compare these results with the energetic ratio ER for plausible medical explanations.

#### 4.1.1 The FFT analysis of the three groups

The figure 7 represent the FFTs' frequency spectrum of one PCG signal from each group, which we used to extract the frequency band (FB) feature.

The table 3 and Figure 8 holds the obtain results of the three groups signals. According to these results, the three groups' frequency band feature is proportional to the ER parameter evolution. In the first group of signals (PCG signals without clicks and murmurs), the IM and COA signals occupy a larger frequency band than the normal case 'N'. At the same time, the COA case FBs' is wider than the IMs'. In other words, the case of an aortic coarctation 'COA' is more intense than a mitral insufficiency 'IM'.

The second and third group of signals (PCG signals with clicks and murmurs) present the same results concerning the FB feature (acceleration of the FB with the increase of the energetic ratio ER). We can also note that the frequency band of pathological cases is greater than of the normal cases [FB of the 3rd group reaches up to 1300 Hz].

#### 4.1.2 The STFT analysis of the three groups

##### 4.1.2.1 Temporal extent feature: $\Delta T$

Figure 9 illustrates de STFT graphic results for the first group of PCG signals. We noted that their temporal representations are similar, whereas the STFT shows differences. Indeed, the temporal extent $\Delta T$ of the second heart sound (S2) is greater than that of the first heart sound (S1) for the three cases (N, IM, and COA) (figure 12, table 4), which we can interpret by the semi-lunar shape of the aortic valves and rapidly closing lungs [32]. We also noticed that the temporal extent of (S1) and (S2) is proportional to the signals' energy of group 1.

The PCG signals of group 2 (PCG signals with clicks) present a direct proportionality of the click segments' temporal extent $\Delta T$ to the energetic ratio (ER) and an inverse one for the heart sounds S1 and S2. The same observation is made for group 3 (PCG signals comprising significant murmurs).

##### 4.1.2.2 Frequency extent feature: $\Delta F$

The first group show a slight decrease in the frequency extent ($\Delta F$) of the first heart sound (S1) and an increase in the second heart sound (S2). Still, the three cases of the first group (N, IM, and CAO) manifest a greater frequency extent of S2 than S1 (table 4 and figure 13).

Regarding the PCG signals of the second group, we note that the presence of clicks affect the heart sounds S1 and S2, where we find a decrease in their frequency extent with an increase in the clicks' $\Delta F$. Yet, both results remain correlated to the energetic ratio ER. From the degree of severity perspective, we could say that the more the frequency extent of the clicks increases, the more the pathological severity evolves.

The presence of murmurs in the thirds group of PCG signals leads to an increase in the frequency extent of both the heart sounds (S1 and S2) and the murmur with a proportional correlation to the energetic ratio evolution. Therefore, the more the frequency extent of the murmurs increases, the more the degree of pathological severity develops.

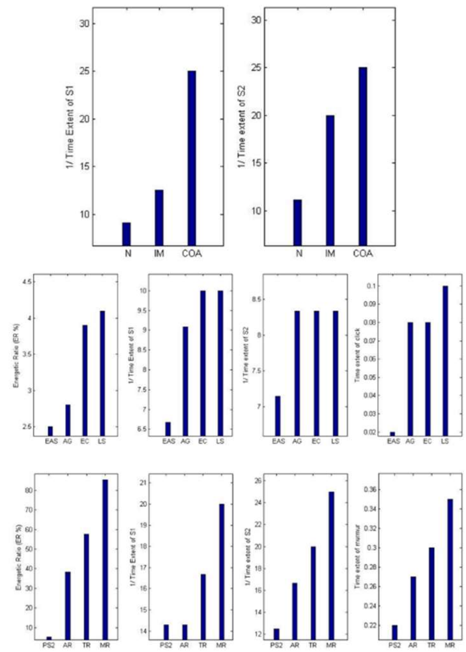

*Figure 12: variation of temporal extent $\Delta T$ in function of : first heart sound (S1), second heart sound (S2), clicks and murmurs for Group 1,Group 2 and Group 3 PCG signals.*

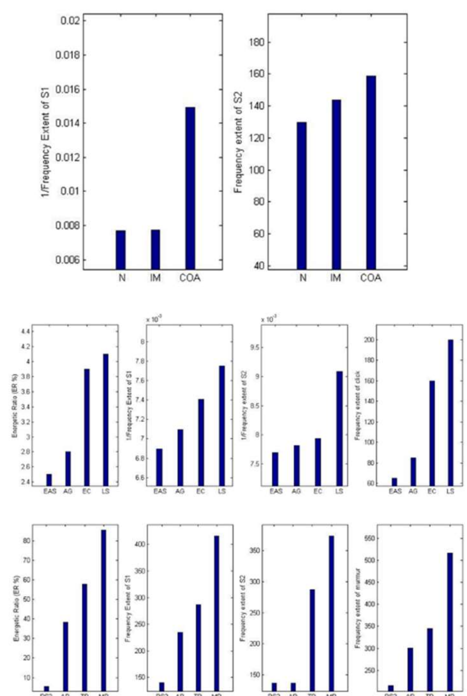

*Figure 13: variation of frequency extent $\Delta F$ in function of : first heart sound (S1), second heart sound (S2), clicks and murmurs for Group 1,Group 2 and Group 3 PCG signals.*

### 4.2 Comparison of the level of severity between the PCG signals of the same pathology (group G4)

Just like for part 1, we analysed the group 4 of PCG signals as mention in table 1 with the FFT and STFT algorithms, we then extracted their relative features and used them to classify our signals from the least sever to the most, afterwards, compared the obtained results to the energetic ratio (ER) evolution.

According to figure 11 and table 5, the frequency band feature (FB) extracted from the FFT analysis shows its ability to monitor the evolution of pathological severity degree. It presents a decrease in values correlated with the increase in energetic ratio ER within the three pathologies (for example: for PCG signals of mitral stenosis (MS), the frequency domain decreases from the case of 'MS1' to the case 'MS4').

The figure 10 represented in the results section illustrates the STFT graphic results for one of the MS (Mitral Stenosis) and MR (Mitral Regurgitation) signals, later found to be the most severe in their signal group.

#### 4.2.1 Temporal extent feature: $\Delta T$

According to the results (figure 14, table 6), the $\Delta T$ of S1 is correlated with the energetic ratio either in an ascending way as for the aortic stenosis and the mitral stenosis signals; Or descending as for the mitral regurgitation signals. On the other hand, the temporal extent of S2 is also correlated to the energetic ratio (ER) either upwards or downwards for the PCG signals of the three pathologies.

The PCG signal murmurs of aortic stenosis show an increase in their $\Delta T$ under the increase of the ER, where this development is a direct indicator of the degree of severity within this pathology [33] (the more $\Delta T$ of the murmurs increases the more the pathological severity of the aortic stenosis develops). Moreover the $\Delta T$ of the mitral stenosis PCG signals (except MS1) and the mitral regurgitation decreases with ER evolution.

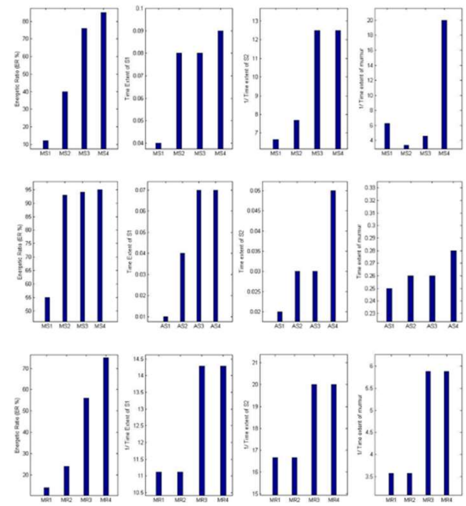

*Figure 14 : variation of temporal extent $\Delta T$ in function of cardiac sound S1 : (a) mitral stenosis (MS),(d) aortic stenosis (AS), (g) mitral regurgitation (MR);of cardiac sound S2: (b) mitral stenosis (MS),(e) aortic stenosis (AS), (h) mitral regurgitation (MR); and murmurs (c) mitral stenosis (MS),(f) aortic stenosis (AS), (i) mitral regurgitation (MR);*

#### 4.2.2 Frequency extent feature: ΔF

The frequency extent ($\Delta F$) of the S1 sound increases for the three cardiac pathologies (figure 15).

In the mitral stenosis case (MS): the first heart sound S1 increased proportionally to the ER evolution, this may be the result of severe mitral stenosis, which includes a loud S1 sound caused by the leaflets of a stenotic mitral valve closing abruptly [34], so we can say that the more the mitral stenosis evolves, the more the S1 increases. However, the frequency extent of S2 and murmurs is inversely correlated to ER (these murmurs can decrease or even disappear when blood flow decreases through the mitral valve [35]).

ISSN: 1992-8645 www.jatit.org E-ISSN: 1817-3195

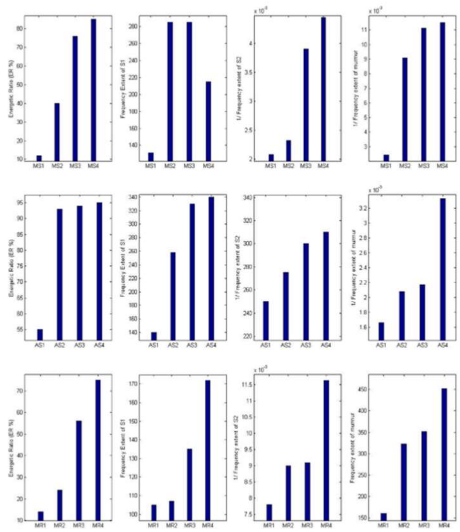

*Figure 15 : variation of frequency extent Δf in function of cardiac sound S1 : (a) mitral stenosis (MS), (d) aortic stenosis (AS), (g) mitral regurgitation (MR); of cardiac sound S2: (b) mitral stenosis (MS), (e) aortic stenosis (AS), (h) mitral regurgitation (MR); and murmurs (c) mitral stenosis (MS), (f) aortic stenosis (AS), (i) mitral regurgitation (MR);*

Concerning the AS group (aortic stenosis), both heart sound S1 and S2 evolve proportionally of the energy ratio. Regarding murmurs, it is the opposite ($\Delta F$ decreases with the RE evolution); which may be due to the decrease in murmur intensity when heart failure develops due to aortic stenosis [33]. .

Regarding the PCG signals of mitral regurgitation (MR), we found that the first heart sound (S1) and the murmurs show an increase in the frequency extent with the evolution of the energetic ratio (ER), while the second heart sound decreases with this evolution.

Hence, all results discussed above remain correlated to the energetic ratio evolution and have a proper medical explanation. Therefore, this comparison of our results with the ER helped us appreciate the features' variation and link it to a plausible medical reason.

Which is the main positive point of these analyses besides there simplicity and speed in term of feature calculation when implemented into more developed signal processing programs.

**4.3 Machine learning results discussion**

As seen in table 7, 99.2% accuracy is achieved when using a combination of spectral and time features (frequency band (FB), frequency extent (ΔF), time extent (ΔT)) to classify the PCG signals in the three main groups.

As we assumed in the introduction, the FFT and STFT technics considered pathological signal morphology similar to a normal (healthy) PCG signal as an unhealthy signal; however, the values of the features somehow remained close to the first group signals. Which, led to a correct classification and a high accuracy value.

When ranking signals according to their severity level (table 8), we achieved a bit lower accuracy (98.9%) than the first.

The problem occurs for signals with a severity level close to the next level. Which may have rather affected the classification process and the accuracy value.

Hence, the classification results shows the efficiency of the STFT and FFT for the phonocardiogram signals classification and that for healthy/clicks/murmurs or severity level discrimination.

To confirm that our comparison to the ER is efficient and consistent, we tested the ability of this feature to classify our database in the two mentioned ways.

Table 9 and 10 results also proves this ability of the energetic ratio parameter (ER) to establish similar classification of the database to a machine learning process with an accuracy of 99.5% and 98.8%. Which is coherent, since the energetic ratio, as mentioned before, refer to the intensity of heart sounds S1, S2 and added sounds (click and murmur) to highlight the dominance of added sounds over heart sounds and to classify the PCG signals according to this dominance. Where [36]

- RE <30% , refers to Light severity level.
- 30% <RE<70%, Moderate severity level.
- RE> 70%, Severe severity level.

As mentioned in the introduction, many research focused on exploiting the FFT and STFT technics for various purposed, like cardiac components identification, pathology discrimination, binary classification etc…. However, with this work, we managed to use the capacities of these technics to classify our PCG signals in two ways:

- According to their pathological origin (normal/morphologically similar, click or murmur).
- According to their severity level (Light, Moderate, and Severe).

Using two approaches:

- The energetic ratio (ER) as a reference parameter, previously used in numerous works [12,19][20-27].
- A machine learning classifier (KNN).

One of the similarities with some of these previous works is the use of the Energetic Ratio ER as a reference feature to compare our results with. Hence, in this work, we started by proving it accuracy before using it for comparison. Which affirms the consistency of our comparison and the previous works using it as a reference feature for PCG signal classification. [12,19][20-27].

Finally, besides ranking a part of our database into the three pre-established groups, the ability of this work to identify the level of severity from a PCG recording and classify it into one of the three named classes using a machine learning process makes the novelty of this paper.

## 5. CONCLUSION:

In closing, Very promising results were obtained in this paper using only two basic methods of signal processing (FFT and STFT) to achieve the assigned objectives, namely the analysis of the pathological severity between different cardiac signals ranked in three pre-established groups, as well as, the severity level evolution of the same pathology (mitral stenosis, aortic stenosis, and mitral regurgitation).

Both approaches used to affirm the obtained results ( K-Nearest Neighbours classifier with FFT/STFT features and Energetic Ratio parameter) allowed us to rearrange a part of our database into three main groups:

- Group 1 (G1): PCG signals having neither click (reduced murmur) nor significant murmur.
- Group 2 (G2): PCG signals with clicks.
- Group 3 (G3): PCG signals with clicks or murmurs.

And successfully classify the remaining database into three classes based on the pathology' severity levels (light, moderate, severe) with high accuracies, 99.2%, 98.9% for the K-Nearest Neighbours classifier with FFT/STFT features and 99.5%, 98.8% for the Energetic Ratio parameter.

Therefore, the energetic ratio ER parameter proved it efficiency for PCG signal classification, which made it a great way to quickly confirm the consistency of an analysis before proceeding with a machine learning classification.

In the end, this study paved the way towards using simple, yet effective, features in cardiac pathologies identification and classification to assist clinicians in critical decision making.

**Acknowledgements**

The authors would like to thank the Directorate-General of Scientific Research and Technological Development (Direction Générale de la Recherche Scientifique et du Développement Technologique, DGRSDT, URL:www.dgrsdt.dz, Algeria) for the financial assistance towards this research.

"**Compliance with Ethical Standards**"

- No, I have nothing to report
- This study was not funded by any party: it is an academic PhD study
- No conflict of interest
- No animal or other used in this study

## REFERENCES

[1]: Shivam Varshney, Satyendra Singh, Computation of Biological Murmurs In Phonocardiogram Signals Using Fast Fourier & Discrete Wavelet Transform, International Conference on Computation, Automation and Knowledge Management (ICCAKM) Amity University, 2020

[2]: Li X et al , Synchronization control of pulsatile ventricular assist devices by combination usage of different physiological signals, Comput Assist Surg 24(sup1):105–112. 2019.

[3]: S. A. Taplidou and L. J. Hadjileontiadis, 'Nonlinear analysis of heart murmurs using wavelet-based higher-order spectral parameters', in *2006 International Conference of the IEEE Engineering in Medicine and Biology Society*, pp. 4502–4505, 2006.

[4]: Ahmad MS, Mir J, Ullah MO, Shahid MLUR, Syed MA, An efficient heart murmur recognition and cardiovascular disorders classification system. Australas Phys Eng Sci Med 42(3):733–743. 2019.

[5]: Watrous R L , Computer-aided auscultation of the heart: from anatomy and physiology to diagnostic decision support Proc. 28th Ann. Int. Conf. IEEE-EMBS 1 140, 2006.

[6]: Akay M, Semmlow J L, Welkowitz W, Bauer M D and Kostis J B , Noninvasive detection of coronary stenoses before and after

angioplasty using eigenvector methods , IEEE Trans. Bio-Med, Eng. 37 1095–104, 1990.

[7]: POTDAR, Ravindra Manohar, *et al,* Optimal Parameter Selection for DWT based PCG Denoising *Turkish Journal of Computer and Mathematics Education (TURCOMAT)*, vol. 12, no 9, p. 3207-3219.2021.

[8]: S.M Debbal and F. Bereksi-Reguig. Second cardiac sound , analysis techniques and performance comparison , Journal of Mechanics in Medicine and Biology (JMMB); ISSN : 0219-5194; 5 (3), September2005.

[9]: T .Omari. Study of aortique stenosis pathological severity degree, magister theses, Tlemcen University, pp 51, 2009.

[10]: R. R.Coifman, Y.Meyer, M. V. Wickerhauser, Wavelet analysis and signal processing. In Wavelets and their applications , Jones and Bartlett, Boston, MA, USA, pp 153-178.1992.

[11]: FATMAWATI, T. Y., YULIANI, A., AFANDI, M. A., *et al,* Comparative Analysis of the Phonocardiogram Denoising System Based-on Empirical Mode Decomposition (EMD) and Double-Density Discrete Wavelet Transform (DDDWT), In : *Proceedings of the 1st International Conference on Electronics, Biomedical Engineering, and Health Informatics*. Springer, Singapore, p. 593-604.2021.

[12]: Baakek, Y. N. E. H., Debbal, I., Boudis, H., & Debbal, S. M. E. A. Study of the impact of clicks and murmurs on cardiac sounds S1 and S2 through bispectral analysis. Polish Journal of Medical Physics and Engineering2021. 27(1), 63-72.

[13]: Sundaram, D. S. B., Damani, D. N., Kapoor, A., Shivaram, S., & Arunachalam, S. P. Deep learning based discrimination of phonocardiogram signal with normal heart sounds and murmur: Feasiblity study. Biomedical Sciences Instrumentation. 2021. 57, 2.

[14]:DEBBAL S.M, Hamza Ch. Pathologies cardiac discrimination using the Fast Fourir Transform (FFT) The short time Fourier transforms (STFT) and the Wigner distribution. J Cardiology Interventions. 2021. 1(1);

[15] S Debbal, F Bereksi-Reguig.,*Spectral analysis of the PCG signals*, The Internet Journal of Medical Technology. Vol 4 N°1.2006.

[16] DEBBAL, S. M., & BEREKSI-REGUIG, F., CARDIAC MURMUR ANALYSIS USING THE SHORT-TIME FOURIER TRANSFORM, Journal of Mechanics in Medicine and Biology, 06(03), 273–284.2006.

[17] S. M DEBBAL- F BEREKSI REGUIG , *The fast Fourier transform and the continuous wavelet transform analysis of the normal and the pathological phonocardiogram"* ; Sciences et Technologies ; ISSN : 1111-5041 , Vol. 17 , pp 81-86.2002.

[18] Abrams,J, Current Concepts of the genesis of heart sounds.I.First and second sounds. ,JAMA, 239-2787. 1978.

[19] Meziani F, Debbal SM, Atbi A, Analysis of phonocardiogram signals using wavelet transform. ,J Med Eng Technol. 2012. 36(6), 283.

[20] Cherif LH, Debbal SM , Adaptive filtering algorithm based on a wavelet packet tree for heart sound signal analysis, Int. J.Med. Eng. Inform. 2018. 10(2), 150

[21] Debbal SM, Hamza C. Heart sounds analysis using the three wavelet transform versions the continuous wavelet transform (CWT) the discrete wavelet transform (DWT) and the wavelet packet transforms (PWT). Journal of Cardiology Interventions. 2021. vol. 1, no 1.

[22] Ahmad TJ, Ali H, Khan SA. Classification of Phonocardiogram using an Adaptive Fuzzy Inference System. In Proc. Int. Conf. Image Process. Comput Vis Pattern Recognit., IPCV 2009, Las Vegas, Nevada, USA, July 13-16, 2009.

[23] Baakek YNEH, Debbal I, Boudis H, Debbal, SMEA. Study of the impact of clicks and murmurs on cardiac sounds S1 and S2 through bispectral analysis. Polish Journal of Medical Physics and Engineering. 2021.27(1) : 63-72.

[24] Berraih SA, Baakek YNEH, Debbal SMEA. Pathological discrimination of the phonocardiogram signal using the bispectral technique. Physical and Engineering Sciences in Medicine. 2020. 43(4), 1371.

[25] Berraih SA, Baakek YNEH, Debbal SMEA. Severity cardiac analysis using the Higher-order spectra. Applied Mathematics and Computation.2021. 409, 126389.

[26] Debbal I, Boudis H, BAAKEK YNEH, Debbal SMEA. Cardiac Pathologies Analysis on the Phonocardiogram Signals Using the Bispectral Technic. International Journal of Advanced Science and Technology. 2020. 29(3), 6764 - 6784.

[27] Berraih SA, Baakek YNEH, Debbal SMEA. Preliminary study in the analysis of the severity of cardiac pathologies using the

higher-order spectra on the heart-beats signals. Polish Journal of Medical Physics and Engineering.2021. 27(1), 73-85.

[28] P.M. Narendra. A branch and bound algorithm for computing k-nearest. IEEE Trans. Comput., 100 (7) (1975), pp. 750-753

[29] Laaksonen, J., Oja, E., 1996. Classification with learning k-nearest neighbors. in: Proceedings of International Conference on Neural Networks (ICNN'96), IEEE, 1996, pp.1480–1483.

[30] Kramer, O., 2013. K-nearest neighbors, . pp.13–23

[31] ARSLAN, Özkan et KARHAN, Mustafa. Effect of Hilbert-Huang transform on classification of PCG signals using machine learning. *Journal of King Saud University-Computer and Information Sciences*, 2022, vol. 34, no 10, p. 9915-9925.

[32] LAMRAOUI H. Characterisation of the phonocardiogram signal. Hadj Lakhdar University. Batna 2. Algeria. 2016.

[33] Xiushui, MD [Internet]. What is the relationship between the systolic murmur and severity of aortic stenosis (AS)?, Medscape [updated 2019 May 7; cited 2023 Jan 19]. Available from: https://www.medscape.com/answers/150638-44363/what-is-the-relationship-between-the-systolic-murmur-and-severity-of-aortic-stenosis-as .

[34] Healio.com [Internet]. Mitral Stenosis - Physical Examination-Topic Reviews [cited 2023 Jan 19]. Available from: https://www.healio.com/cardiology/learn-the-heart/cardiology-review/topic-reviews/mitral-stenosis/physical-examination

[35] Guy P. Armstrong , MD [Internet]. Waitemata Cardiology, Auckland Valvular Disorders, MSDManuals [updated 2022 sep ; cited 2023 Jan 19]. Available from: https://www.msdmanuals.com/professional/cardiovascular-disorders/valvular-disorders/mitral-stenosis.

[36] Debbal S, Bereksi-Reguig F. Analyse spectro-temporelle des bruits cardiaques par les transformees discrete et continue d'ondelettes. Sciences & Technologie. B, Sciences De l'ingénieur. 2005(23):5-15.